Two-photon above-threshold ionization using extreme-ultraviolet harmonic emission from relativistic laser–plasma interaction

2012 New J. Phys. 14 043025

(http://iopscience.iop.org/1367-2630/14/4/043025)

New Journal of Physics
The open-access journal for physics

Two-photon above-threshold ionization using extreme-ultraviolet harmonic emission from relativistic laser–plasma interaction

P Heissler[1,6], P Tzallas[2], J M Mikhailova[1,4], K Khrennikov[1], L Waldecker[1], F Krausz[1,3], S Karsch[1,3], D Charalambidis[2,5] and G D Tsakiris[1]

[1] Max-Planck-Institut für Quantenoptik, D-85748 Garching, Germany
[2] Institute of Electronic Structure and Laser, FORTH, GR-71110 Heraklion (Crete), Greece
[3] Fakultät für Physik, Ludwig-Maximilians-Universität München, D-85748 Garching, Germany
[4] A M Prokhorov General Physics Institute, Russian Academy of Science, 119991 Moscow, Russia
[5] Department of Physics, University of Crete, GR-71003 Heraklion (Crete), Greece
E-mail: info@patrick-heissler.de

New Journal of Physics **14** (2012) 043025 (9pp)
Received 23 December 2011
Published 20 April 2012
Online at http://www.njp.org/
doi:10.1088/1367-2630/14/4/043025

Abstract. We report on the observation of energy-resolved photoelectron (PE) spectra produced via two-extreme-ultraviolet-(XUV)-photon above-threshold ionization (ATI) of argon atoms. The XUV radiation consists of higher-order harmonics generated by the process of the relativistic oscillating mirror (ROM) in high-peak-power laser–pulse interaction with solid targets. The energetic XUV radiation is focused into an argon gas target at intensities high enough to induce two-photon ionization at yields that allow the recording of energy-resolved PE spectra. A clear two-XUV-photon ATI PE peak structure is observed in shot-to-shot measurements. This work is a first step towards a frequency-resolved optical gating-type characterization of attosecond pulse trains emanating from relativistic laser–plasma interactions and thus is important for XUV-pump–XUV-probe applications of these harmonics.

[6] Author to whom any correspondence should be addressed.

Contents

1. Introduction

Recent and anticipated developments in short-pulse high-peak-power laser technology open up new perspectives for *intense* extreme ultraviolet (XUV)/x-ray attosecond (asec) radiation sources [1]. A measure of the term 'intense' is the ability to observe nonlinear processes induced exclusively by XUV radiation. Once this regime has been reached, unique tools for asec pulse metrology and also for pump–probe applications will be available. Indeed, during the last decade, sources based on higher harmonic generation in gaseous media have reached intensity levels that have allowed the observation of two-XUV-photon ionization induced by a superposition of harmonics [2–4]. This achievement culminated in the use of the second-order intensity volume autocorrelation (2-IVAC) technique [5, 6] to directly visualize asec pulse trains [7, 8]. The advancement of this technique led to energy resolved [9, 10] as well as to interferometric [11] second-order autocorrelation (AC) measurements of asec pulse trains. Very recently, progress in the generation of energetic XUV super-continua [12, 13] has allowed the observation and utilization of two-XUV-photon processes induced by quasi-isolated pulses with durations lying between 0.8 and 1.7 fs [14].

However, inherent limitations in the harmonic generation process in gases due to the depletion of the gas medium put a ceiling on the maximum achievable yield of XUV radiation. In contrast, harmonic generation from solid density targets with superior phase properties [15, 16] exhibits no fundamental limit for the maximum laser intensity that can be used [17] and thus presages unprecedented asec pulse energies [17, 18]. Currently, frequency up-conversion of laser light in the plasma medium holds the record in emitted energy per pulse of 40 μJ at the source [19]. This has been promptly exploited in an experiment using two-XUV-photon ionization induced by harmonics from solid targets to confirm sub-fs confinement of the XUV radiation in a pulse train [19].

Like any second-order AC approach, 2-IVAC provides an acceptable estimation of the pulse duration but no information about the temporal profile of the pulses. For optical frequencies, extension of the second-order AC approach to energy-resolved detection of the interaction products provides additional data required by the frequency-resolved optical gating (FROG) technique [20] to attain full spectral phase retrieval of the pulse. The information obtained through the FROG technique combined with the measured spectral amplitude distribution allows a complete reconstruction of the pulse profile, with the sole ambiguity of left–right asymmetry. In the XUV spectral region, a FROG-type approach can be implemented by recording energy-resolved ionization, i.e. energy-resolved electron spectroscopy. A vacuum ultraviolet (VUV) ($\lambda = 160$ nm) FROG-type measurement has been carried out for a single

harmonic [21]. Attosecond pulse metrology will benefit considerably from an extension of this approach to several harmonics. An essential prerequisite here is an observable energy-resolved two-XUV-photon ionization, an extraordinary challenge at currently available XUV intensities. Thus, while for asec pulse trains emitted by gases this type of measurement is rare [10, 22], for their counterpart from surface plasma harmonics it is to date entirely missing. This is because it is only recently that a two-XUV-photon ionization by surface plasma harmonics has been made possible [19]. An additional difficulty arises from the presence of both even and odd harmonics, while gases emit only odd harmonics. This impedes the observation of well-resolved PE peaks.

In this paper, we report on the first measurement of energy-resolved electron spectra in a non-resonant two-XUV-photon ionization of Ar atoms. The ionization process is induced by harmonics due to the ROM process from laser–plasma interaction [17]. A clear multi-peak PE spectral structure, with energy spacing equal to the laser photon energy corresponding to the absorption of two photons from different harmonics, is observed in single-shot measurements. The structure, although blurred, is clearly visible in averaged spectra as well. The present result represents an important step towards detailed pulse metrology and time domain investigations based on intense plasma–vacuum interface harmonics.

2. The experimental setup

The experiment was performed using the 100 TW Ti:sapphire laser system of the Max Planck Institute of Quantum Optics, which delivers laser pulses of 26 fs duration, with energy of $\sim$2 J per pulse, at 5 Hz repetition rate and a central wavelength of 800 nm. The measured contrast of the laser pulse was 10^{11} at ns time scales and 10^{7} at 3 ps before the pulse peak. In the actual experiment the laser energy on the target was $\sim$100 mJ per pulse, as at this energy level the best conversion efficiency, harmonic spectral distribution and spatial coherence of XUV emission were achieved. This can be attributed to an optimum pre-plasma to intensity relation at this energy level, a pivotal parameter in ROM harmonic generation.

The experimental setup is shown in figure 1. The p-polarized laser beam was focused by an $f/2.5$, 90° off-axis parabolic mirror (PM1) on a 1 cm thick fused silica target (ST) of 12 cm diameter. The angle of incidence on the target was 45°. The $f/2.5$ parabolic mirror was coated with a layer of enhanced silver having an effective focal length of 20 cm. In every shot, a single laser pulse interacted with a new (unused) position of the target. This was accomplished by precision rotational and translational motorized stages that rotated the target substrate after each shot and linearly translated it parallel to its surface after every full rotation. Full control over the position and pointing of the laser beam was achieved by controlling the x, y, z, and the tip and tilt degrees of freedom of the focusing parabola.

Adjustment of the laser focus was possible by moving the entire target setup out of the laser beam. Removal occurred through an additional long linear translation stage. A microscope objective (IL1) connected to a 14 bit camera could then be moved in the beam path, allowing the observation of the laser focus.

The diverging harmonic radiation, generated on the target and co-propagating with the laser beam in the specular direction, was collimated by a 135° off-axis fused silica parabolic mirror (PM2) having a focal length of 13 cm. This mirror was placed on a motorized translation stage, so that it could be moved out of the beam, allowing it to enter a home-built imaging spectrometer (S) equipped with a 1200 lines mm^{-1} Hitachi flat-field grating.

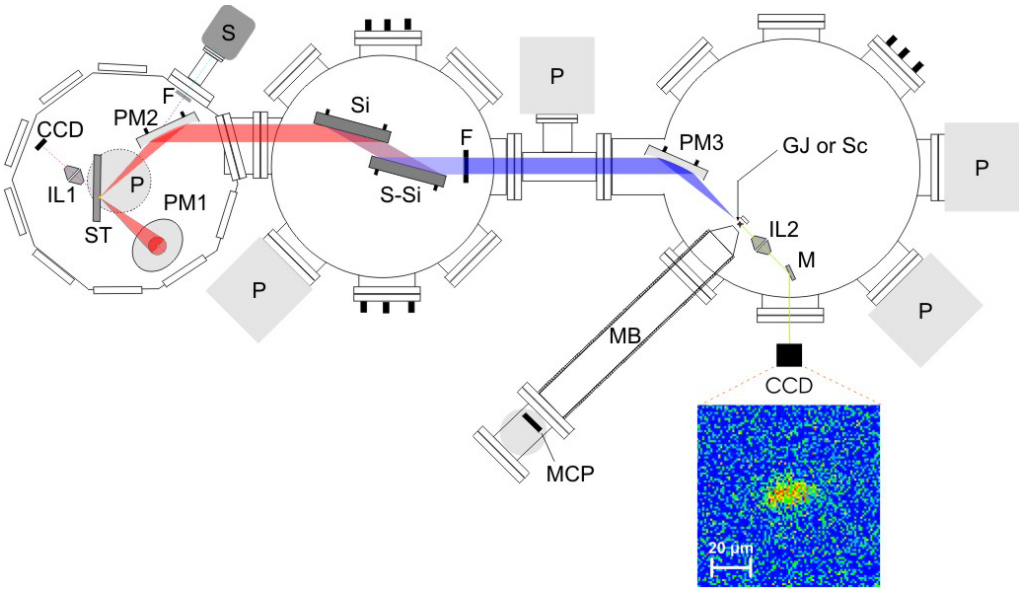

Figure 1. Schematic diagram of the experimental setup. **PM1, 2, 3**: parabolic mirrors; **ST**: solid target; **IL1, 2**: imaging systems; **F**: filters; **S**: XUV flat field spectrometer; **S-Si, Si**: silicon plates; **GJ**: Ar gas jet; **Sc**: the scintillator used for the imaging of the XUV focus (the image in the inset); **MB**: 1.5 m long magnetic bottle; **MCP**: microchannel plates; **M**: mirrors; **P**: turbo pumps.

By placing the 135° off-axis parabola in the beam path, the collimated beam was directed to a second vacuum chamber. In this chamber, two Si plane mirrors placed at Brewster's angle for $\lambda = 800$ nm reflected the XUV radiation, thus separating it from the absorbed IR laser beam. The XUV spectral region used in this experiment was selected by a 150 nm thick Sn filter. The filtered XUV radiation entered a third chamber, in which it was focused by a second 135° parabolic mirror (PM3) into a pulsed argon gas jet. The overall transmission of the setup is estimated to be higher than 0.25% for the spectral region transmitted by the filter [23]. In a separate experiment under similar conditions described in detail in [23], the XUV spot size was assessed to be $\sim$16 μm and the IR–XUV conversion at the target was conservatively estimated as 5×10^{-5}. Thus the XUV energy per laser pulse at the interaction area of the third chamber is $\sim$25 nJ, which when focused to a spot of $\sim$16 μm diameter resulted in a lower limit for the focused intensity of 5×10^{11} W cm^{-2}.

A 1.5 m long magnetic bottle (MB) electron spectrometer was attached to the third chamber with its axis perpendicular to the beam propagation axis (see figure 1). The MB was used in order to record energy-resolved PE spectra produced through two-photon ionization of argon. The energy resolution of the spectrometer ($\Delta E/E \approx 3\%$) is high enough to distinguish peaks originating from the absorption of different combinations of two harmonic photons leading to different energy positions in the continuum, while its 2π collection solid angle substantially improves the electron collection efficiency with respect to our previous relevant experiments [22]. In order to maximize the collection efficiency of the MB, a 10 V repelling voltage was applied between a repeller plate and the spectrometer entrance in the interaction region. This voltage repels towards the detector the part of the single-XUV-photon ionization

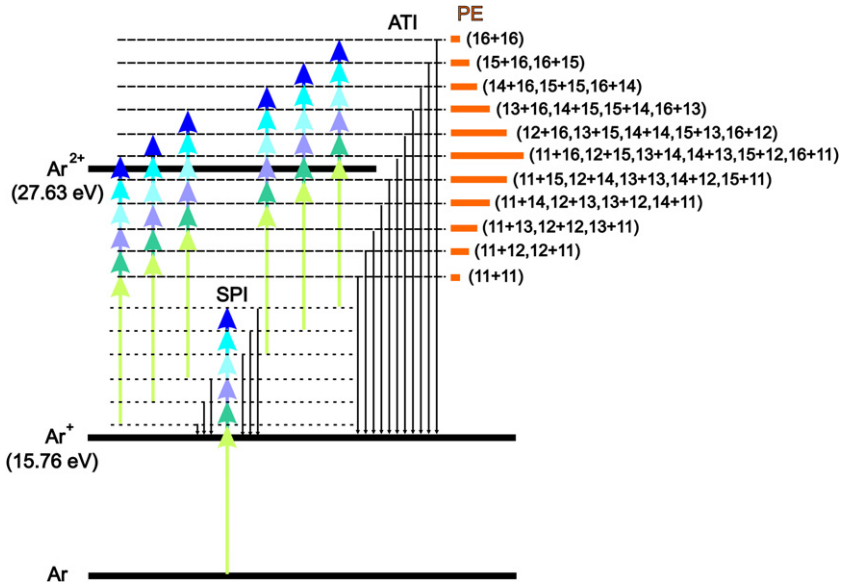

Figure 2. Ionization scheme of Ar indicating the various harmonic photon combinations contributing to the ATI peaks.

PEs originally emitted in the backward (away from the detector) direction. These electrons arrive at the detector after those ejected towards the detector and have been used to deduce the energy of the XUV radiation.

3. Results and discussion

Figure 2 illustrates the ionization scheme of Ar in this experiment. The ionizing radiation consists of harmonics 11th–16th. Single-photon absorption of this harmonic comb leads to single-photon ionization (SPI) of Ar, producing a series of six PE peaks separated by the photon energy of the driving laser field. Absorption of a second photon of the harmonic comb prior to the formation of Ar ions leads to one- or two-color above-threshold ionization (ATI). Different combinations of harmonic photons lead to the same excess energy and thus contribute to the same ATI peak. To the lowest- and the highest-energy ATI peak (excess energy $22\hbar\omega_{\text{laser}}$-IP and $32\hbar\omega_{\text{laser}}$-IP, respectively, with $\hbar\omega_{\text{laser}}$ being the laser photon energy and IP the ionization potential of Ar), only the 11th or the 16th harmonics, respectively (two ionization channels respectively) contribute. To the second lowest- and the second highest-energy peak (excess energy $23\hbar\omega_{\text{laser}}$-IP and $31\hbar\omega_{\text{laser}}$-IP, respectively), two combinations of harmonics (11th+12th, 12th+11th) and (15th+16th, 16th+15th) and two ionization channels, respectively, contribute. To the third lowest- and the third highest-energy peak (excess energy $24\hbar\omega_{\text{laser}}$-IP and $30\hbar\omega_{\text{laser}}$-IP, respectively), three combinations (four channels) of harmonics, respectively, and so on, contribute. To the central ATI peak (excess energy $27\hbar\omega_{\text{laser}}$-IP), six combinations of harmonics and six ionization channels contribute. All these processes are two-photon processes and thus may be used in the performance of energy-resolved second-order AC measurements. These measurements, subject to the fluctuation level of the signal, may potentially be exploited as an input to a FROG-type determination of the temporal profile of the harmonics waveform. Some combinations of the two-photon absorption lead also above the second ionization threshold,

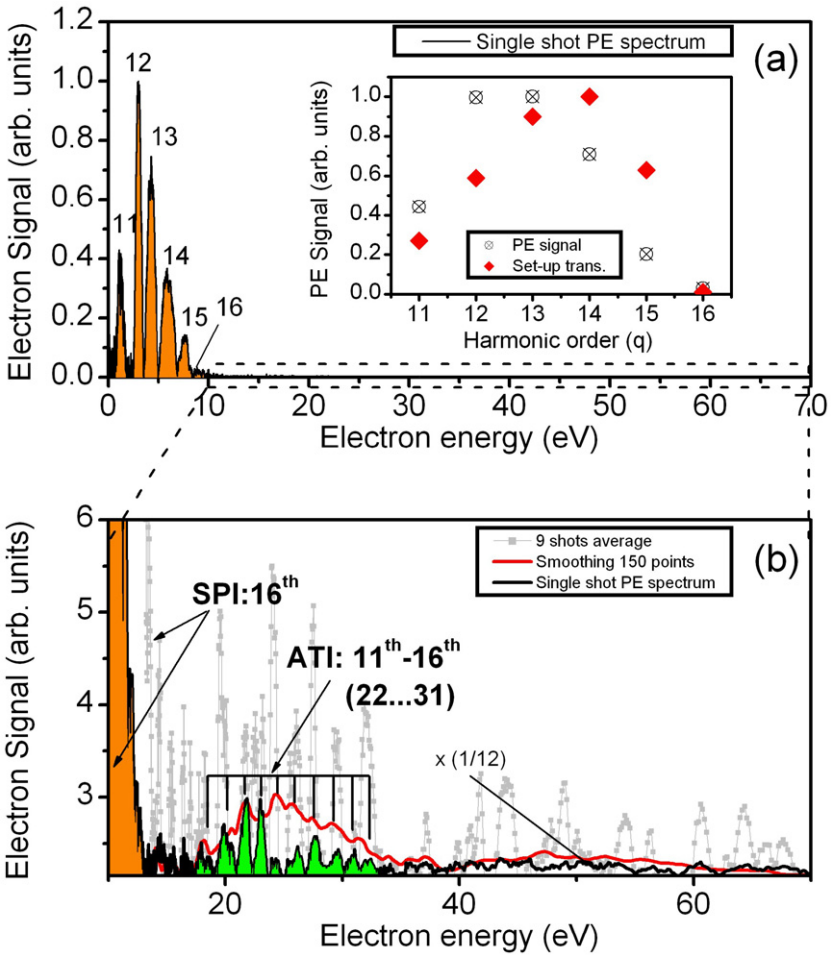

Figure 3. Single- (SPI) and two-XUV-photon ionization (ATI) spectra of Ar. (a) Background-corrected single-photon PE spectrum of Ar (black line). The measured (crossed circles) and calculated (red rhombs) overall spectral transmission of the setup is shown in the inset. (b) Two-XUV-photon ATI PE spectrum of Ar. The black line filled in green shows a single-shot trace, the gray dotted line is an average of nine shots and the red line is obtained from the nine shots average (gray dotted line) after a 150 points moving average is performed. The orange and green shaded areas depict the SPI and ATI signals, respectively.

i.e. to two-photon direct double ionization (TPDDI) of argon. This process produces low-energy electron continua in the energy range of the SPI. Due to the significantly lower rate of the TPDDI processes as compared with the SPI, it will have a negligibly low contribution to this energy range of the PE spectrum. Two-photon sequential double ionization (SDI), i.e. the formation of Ar^+ followed by its ionization leading to Ar^{2+}, requires photon energies >27.63 eV. For the set of harmonics of this experiment, the SDI process becomes a three-photon process and thus it represents a negligible contribution to the double ionization of Ar.

Measured PE spectra are shown in figure 3. Figure 3(a) depicts a wide energy range spectrum, in which the dominant contribution is that of SPI. The spectrum is a single laser shot

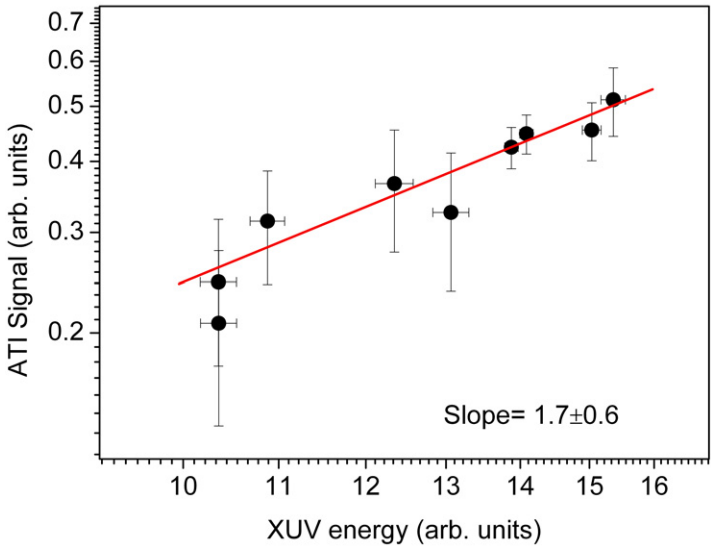

Figure 4. Total ATI PE yield as a function of the XUV energy. The energy of the XUV radiation was deduced from the 'back reflected' single-XUV-photon PE signal after applying a −10 V repelling electric field in the interaction region.

record. A clear peak structure corresponding to the single-photon absorption of the 11th–16th harmonics is observable. Each point (crossed circle) in the inset of figure 3(a) is the area of each peak of the electron spectrum (spectrally integrated signal). Thus the distribution in the inset corresponds to the spectral intensity distribution of the harmonic spectrum at the Ar target. The red rhombs show the overall spectral transmission of the setup used, which is in reasonable agreement with the measured data.

Figure 3(b) shows the part of the spectrum above 10 eV, i.e. above the overwhelming SPI peak area, thus allowing the observation of low-peak-height structures. The black line (filled green area) shows a single-shot spectrum consisting of ten peaks with energies ranging from $22\hbar\omega_{\text{laser}}$-IP to $31\hbar\omega_{\text{laser}}$-IP. Those are exactly the energies expected from a two-photon ATI caused by combinations of the 11th–16th harmonics. The peak with the highest possible energy of $32\hbar\omega_{\text{laser}}$-IP is not clearly observable due to the low intensity of the 16th harmonic. In figure 3(b), the gray points depict a spectrum obtained by averaging the data from nine laser shots, while the green filled curve is a single-shot record of the PE spectrum. In order to clearly demonstrate the reproducible occurrence of the ATI PE peaks, we have processed the average signal over nine shots (gray points) by performing a 150-point moving average on the data (red curve). It is seen that despite the shot-to-shot fluctuations, the PE peaks in the smoothed average record emerge at the same position as in the single-shot record (green filled curve). This proves that the PE peaks are indeed the ATI peaks due to the harmonic photon combinations indicated in figure 2.

From the measured peak positions, it is clear that the underlying process is a two-photon ATI process. The basis for drawing this conclusion is the measured dependence of the integrated electron signal of these peaks on the energy of the ionizing XUV radiation, as shown in figure 4. Due to the low signal level, the error of the measure data and that of the slope of the linear fit in the log–log diagram are large. The measured slope is 1.7 ± 0.6, which within the error is an indication of a two-photon process.

4. Conclusions

We have reported on the measured energy-resolved ATI spectra of Ar produced during the interaction of Ar atoms with intense XUV harmonics emanating from solid density plasmas, driven by the relativistic interaction of laser radiation with a solid surface. The measured spectra consist of two parts: a low-energy part, where photo-peaks are produced through SPI of Ar and a high-energy part, the low-amplitude peaks, which result from two-XUV-photon ATI of Ar. The demonstration of observable two-XUV-photon ATI is an important step towards advanced applications of harmonics emitted from surface plasmas. Two-XUV-photon ATI allows extension of the 2-IVAC approach to shorter wavelengths than those used so far. It is, furthermore, the process on which a FROG-type characterization of asec pulses will be based. In addition to the applications envisaged in pulse metrology, two-XUV-photon ATI allows the detailed study of ultrafast above-threshold dynamics. This work paves the way for the accomplishment of these goals, an endeavor that will be greatly facilitated by further progress in the development of XUV sources.

Acknowledgments

This work was supported in part by the DFG project TR-18 and the MAP excellence cluster, by the Laserlab-Europe, grant number 228334, and by the association EURATOM–MPI für Plasmaphysik. This work was also supported by the European Commission programs ULF, ALADIN (grant number 228334), ATTOFEL (grant number 238362), FASTQUAST (PITN-GA-2008-214962) and CRISP (grant number 283745) and by the FLUX program (PIAPP-GA-2008-218053) of the 7th FP. The work was performed in the framework of the IKYDA program (no. 177) for the promotion of scientific cooperation between Greece and Germany from which partial financial support was also partially obtained. JMM gratefully acknowledges financial support from the Alexander-von-Humboldt Foundation and the RFBR grant numbers 08-02-01245-a and 08-02-01137-a.

References

[1] Krausz F and Ivanov M 2009 *Rev. Mod. Phys.* **81** 163
[2] Kobayashi Y *et al* 1998 *Opt. Lett.* **23** 64
[3] Kobayashi Y *et al* 2000 *Appl. Phys.* B **70** 389
[4] Papadogiannis N A *et al* 2003 *Phys. Rev. Lett.* **90** 133902
[5] Tzallas P *et al* 2005 *J. Mod. Opt.* **52** 321
[6] Faucher O *et al* 2009 *Appl. Phys.* B **97** 505
[7] Tzallas P *et al* 2003 *Nature* **426** 267
[8] Nikolopoulos L A A *et al* 2005 *Phys. Rev. Lett.* **94** 113905
[9] Miyamoto N *et al* 2004 *Phys. Rev. Lett.* **93** 083903
[10] Nabekawa Y *et al* 2006 *Phys. Rev. Lett.* **96** 083901
[11] Nabekawa Y *et al* 2006 *Phys. Rev. Lett.* **97** 153904
[12] Tzallas P *et al* 2007 *Nature Phys.* **3** 846
[13] Skantzakis E *et al* 2009 *Opt. Lett.* **34** 1732
[14] Tzallas P *et al* 2011 *Nature Phys.* **7** 781
[15] Dromey B *et al* 2006 *Nature Phys.* **2** 456
[16] Quéré F *et al* 2008 *Phys. Rev. Lett.* **100** 95004

[17] Tsakiris G D *et al* 2006 *New J. Phys.* **8** 19
[18] Baeva T *et al* 2006 *Phys. Rev.* E **74** 046404
[19] Nomura Y *et al* 2009 *Nature Phys.* **5** 124
[20] Trebino R and Kane D J 1993 *J. Opt. Soc. Am.* A **10** 1101
[21] Sekikawa T *et al* 2002 *Phys. Rev. Lett.* **88** 193902
[22] Benis E P *et al* 2006 *New J. Phys.* **8** 92
[23] Waldecker L *et al* 2011 *Plasma Phys. Control. Fusion* **53** 124021